Excerpt from the Proceedings of the 2011 COMSOL Conference in Stuttgart

Super-Lattice Effects in Ordered Core-Shell Nanorod Arrays Detected by Raman Spectroscopy

A. Alabastri*[1], R. Krahne[1], A. Giugni[1], G. Das[1], R. Zaccaria[1], M. Zanella[1], I. Franchini[1] and E. di Fabrizio
[1]Italian Institute of Technology (IIT), Via Morego 30, 16163, Genoa, Italy
*Corresponding author: alessandro.alabastri@iit.it

Abstract: We studied the optical phonon excitations (LO) of ordered arrays of dot/ rod core-shell CdSe/ CdS nanorods by Raman spectroscopy. Upon deposition on planar substrates the nanorods formed super-lattice structures via side-by side assembly into tracks over some microns of length.
COMSOL Multiphysics software has been used to calculate the magnitude of the electric field generated by the interaction of an incident electromagnetic wave with an array of CdSe/CdS nanorods. In particular two configurations were considered: i) localized charges in the nanorods; ii) no localized charges in the nanorods. To this purpose a 2D model has been implemented and simulations have been performed for both polarizations of the incident electromagnetic field. Multiphysical characteristics of COMSOL have been exploited as the simulation relied on a two-steps process. First, localized charges have been set-up near the CdSe cores to mimic the promotions of electrons and an electrostatic simulation was launched. Second, the calculated electric displacement field was used to modify materials conductivity and thus the interaction with the impinging electromagnetic wave.

Keywords: Super-Lattice effect, Nanorods, Raman, electromagnetic interaction, electrons promotion.

1. Introduction

Ordered self-assembled nanocrystal arrays are of great interest for both basic science and practical applications. They promise novel physical properties due to collective effects and provide a cost effective way to fabricate macro-scale devices that rely on the peculiar properties of their individual components. Nanorods are especially appealing in this respect because their elongated shape results in distinctive properties like linearly polarized emission and orientation dependent conductivity, which were observed both on the single particle level [1-3] and on large scale assemblies [4-6]. Super-lattice effects like current oscillations have been detected in track-like assemblies of CdSe nanorods. [7] The vibrational modes (phonons) of nanocrystals can have significant impact on their optical and electrical response as manifested by phonon replicas in the emission spectrum [8] and by phonon-assisted charge tunneling in electron transport experiments on single nanorods [9]. Optical phonons in colloidal spherical and rod-shaped nanocrystals have been studied in detail, revealing a red-shift and broadening of longitudinal-optical (LO) phonon peak due to confinement effects [10]. Higher harmonics of the LO phonons allowed to evaluate the coupling strength which is commonly expressed by the Huang Rhys factor [11-12]. The surface-optical (SO) phonon modes were found to depend on the aspect ratio of the nanorods [13-14], and radial breathing modes have been observed both in spherical and rod-shaped nanocrystals [15-16]. Linearly polarized Raman experiments on oriented arrays of CdSe nanorods allowed to distinguish LO phonon modes oscillating parallel and perpendicular to the nanorod axis [13, 17]. Novel physical properties arising from the superstructure of the ordered nanocrystal assemblies have been reported, for example, by scanning tunneling microscopy, where a reduced band gap was observed in densely packed arrays. [18-19]

2. Methods

In this work we report Raman experiments on core-shell CdSe/CdS nanorods with a dot-in-a-rod architecture that self-assembled into micron size tracks. In addition to the confined LO phonon modes of the CdSe and CdS materials we observed a broad phonon mode that appeared at a slightly lower energy than the LO phonon of the CdS shell. This mode was in resonance with the exciton transitions of the CdSe core and could not be detected in disordered nanorod assemblies. We attribute its appearance to a grating coupler effect that was generated by the photo-excited charges in the super-lattice formed by the nanorod tracks, giving access to the LO phonon dispersion at higher wave vector k. A calculation of the

modulation of the electric field vector **E** of a plane electromagnetic wave caused by the photo-induced charges supported our assumption. Grating coupler effects in ordered arrays of highly luminescent nanocrystals could be very interesting for coupling excitons to other nanocrystal excitations like phonons and plasmons. [20]

The nanorods were fabricated by the seeded growth method according to Ref. [4]. We investigated nanorods with lengths from 30 to 50 nm and core sizes ranging from 2.5 to 3.2 nm and we will present in the following the data obtained from two typical samples named „A" and „B" (Figure 1), which had a diameter of around 5 nm, and a length of 40 and 30 nm, respectively. Optical absorption and emission spectra were recorded from nanorod solutions with a commercial spectrophotometer. The tracks represent a nanorod superlattice in which the lattice period is given by the rod diameter. Microprobe Raman (Horiba, T64000, in subtractive configuration) experiments were performed under ambient conditions using an Argon-krypton ion laser (Spectra-Physics, Ar:Kr *Stabilite 2018 –RM*) at 458 nm, 488 nm, and 514 nm. The inelastic scattered radiation from the substance was filtered by triple-monochromator, equipped with 1800 lines/mm grating, and the output signal was detected by peltier-cooled CCD detector. The samples were mounted on an inverted microscope (Olympus, IX71) and an aplanatic, infinity-corrected, microscope objective 100X (Olympus, UPLSAPO) was employed to focus laser excitation to a diffraction-limited spot and to collect the back-scattered Raman signal.

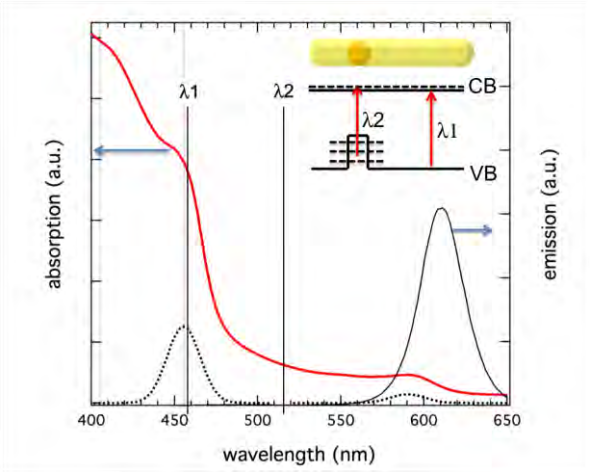

Figure 2. Absorption and emission spectra of CdSe/CdS nanorods with 30 nm length and a core size of 3 nm (sample B) recorded from solution. Gauss fits to the first absorption peaks from the CdSe core and CdS shell are shown by the dotted lines. Two excitation wavelengths for the Raman experiments (λ1=458 nm and λ2=514 nm) are marked by the vertical lines. The inset illustrates the dot/rod core-shell architecture and the related band structure of the nanorods. At a wavelength of 514 nm only transitions related to the CdSe are possible.

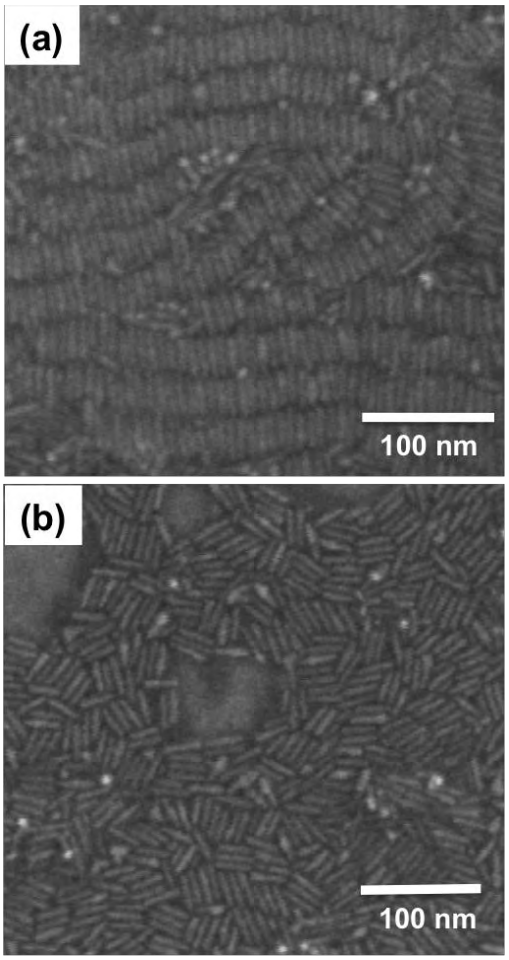

Figure 1. (a) Scanning electron microscopy (SEM) image of nanorod tracks (sample track A) formed by drop deposition of the nanorod solution on a Si substrate followed by solvent evaporation under ambient conditions. (b) SEM image of disordered nanorods.

3. Experimental Results

Absorption and emission spectra of core-shell nanorod sample B (for data from sample A see supporting information) are reported in Fig. 2. Gauss fits to the relevant sections of the absorption spectrum revealed the lowest absorption peak of the CdSe core at 590 nm and of the CdS shell at 455 nm, both with a FWHM of 15 nm. The emission peak at 610

nm is red-shifted with respect to the CdSe core absorption due to the Stokes shift [4, 21]. The excitation wavelengths employed in the

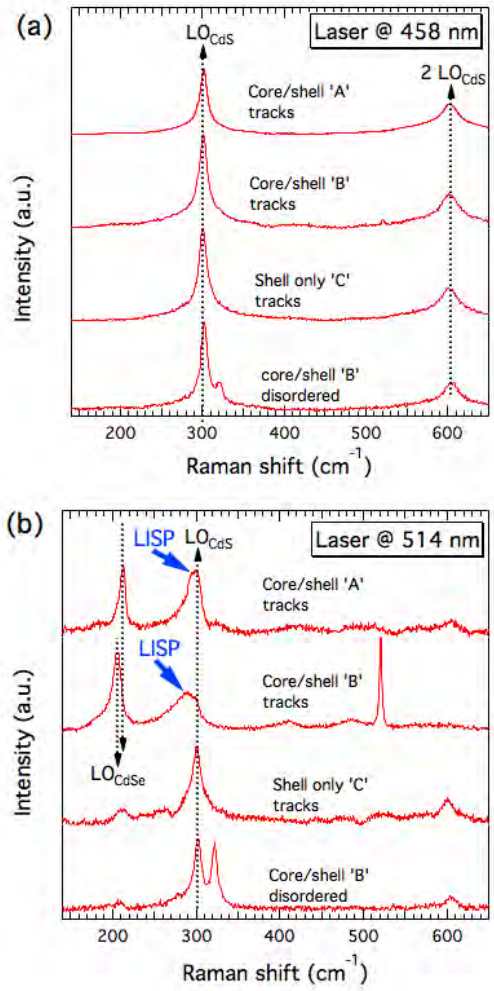

Figure 3. Raman spectra recorded from different nanorod films at an excitation wavelength of 458 nm (a) and 514 nm (b). The light-induced-superlattice-phonon (LISP) mode is indicated by the blue arrows. The peaks at 322 cm^{-1} and 521 cm^{-1} originate from the CaF_2 and Si substrates, respectively.

Raman experiments are indicated by the black vertical lines. The inset of Fig. 2 illustrates the core-shell architecture, in which a spherical CdSe core is embedded in a rod-shaped CdS shell, as well as the related band structure, where we assumed strong confinement for the holes in the valence band, and a small offset in the conduction band. [22-23] Typically, the Raman signal of the LO phonon excitations is resonant with the excitonic transitions [11, 24]. Therefore, at the excitation wavelength $\lambda 1$=458 nm the Raman signal is in resonance with the transitions in the nanorod shell (CdS), while at $\lambda 2$=514 nm it is in resonance with transitions related to excited states in the CdSe core [4] (see red arrows in the inset of Fig. 2). Figure 3a shows Raman spectra of the nanorod samples at an excitation wavelength of 458 nm, i.e. in resonance with the CdS shell states. We observed a strong Raman peak at 302 cm^{-1} that corresponds to the CdS LO phonon, slightly red shifted from the CdS bulk value (305 cm^{-1} [25]) due to confinement effects [10]. Also the first overtone of the CdS LO phonon at 604 cm^{-1} can be identified. We conclude that at an excitation wavelength of 458 nm, apart from very small differences in the LO phonon line shape, no generically different behavior from the different nanorod samples was observed. The Raman spectra in resonance with the higher exciton transitions of the CdSe core are depicted in Fig. 3b. Here, in addition to the CdS mode, we also observed the CdSe LO phonon due to the strong resonance with the core transitions. Close inspection of the CdSe phonon peak position and width from samples „tracks A" and „tracks B" reveals a different magnitude of the red shift due to the confinement effects. The CdSe LO phonon of the sample „tracks B" , which emits at 610 nm (same as in Fig. 2), is more red shifted than that of the sample „tracks A" emitting at 630 nm, in good agreement with the expected LO phonon confinement effects.[10] The most interesting feature in Fig. 3b is the broad Raman peak at 295 cm^{-1} (marked "LISP") that was only observed from the nanorods assembled into tracks, i.e. from samples where the nanorods were assembled into a superlattice, and only at an excitation wavelength in resonance with the excited states of the CdSe core. Neither disordered core-shell nanorods, nor ordered nanorods consisting of CdS only manifested this broad Raman mode, as demonstrated in Fig 3b. Furthermore, we can exclude that the „LISP" peak is due to SO phonon modes since the SO phonon energy should be at much lower energy.

4. Discussion of Results

The peculiar resonance of the broad LISP peak, which occurred in the range of CdS phonon energy dispersion, was in resonance with electronic transitions of the CdSe core. Since this mode is only observed in spectra from the nanorod tracks, we can attribute its origin to a super-lattice effect.

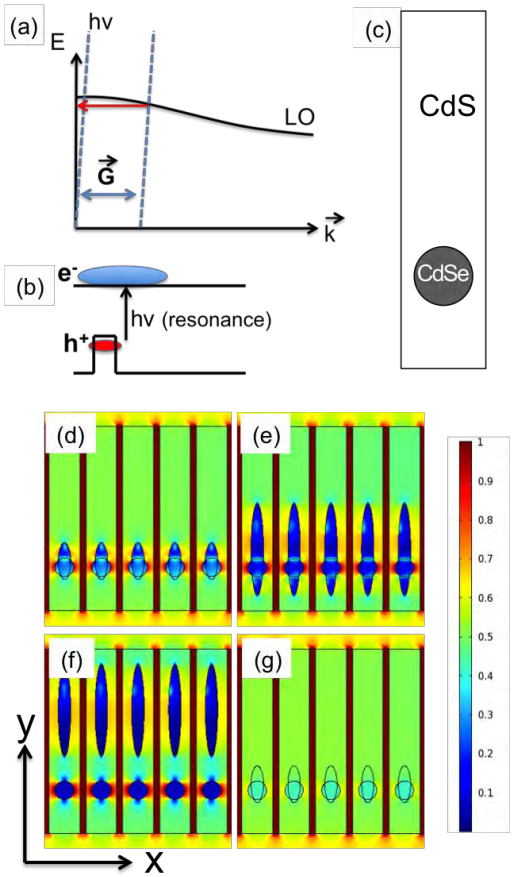

Figure 4. (a) Illustration of the negative LO phonon dispersion at the Γ-point in CdS and the grating coupler effect that allows the light to interact with regions at higher wave vector k. In our case the superlattice period *a* is approximately 5 nm (given by the rod diameter), while the crystal lattice constant in CdS is around 0.5 nm. Therefore $G=2\pi/a$ corresponds to about $1/10^{th}$ of the Brillouin zone of CdS. (b) Scheme illustrating the distribution of photo-induced charges in a core-shell nanorod upon light excitation with energy below the CdS band gap. (c) Material and shape that were used for the calculation in d-g. (d-g) Calculated in-plane component **E** of the electric field of an electromagnetic wave in an array of nanorods, (d-f) with photo-induced charges and (g) without photo-induced charges. The scale bar in V/m refers to the color coding in (d-g). One of the assumed spatial distributions of electrons and holes with small (d) and relatively large (e) electron delocalization should describe our system well. Complete charge separation (g) would lead to an even stronger E-field modulation

The LO phonon dispersion in CdS (and CdSe for that matter) that leads to a red-shifted superlattice phonon mode is illustrated in Figure 4a. We see that a broad and significantly red-shifted phonon mode can be explained by the negative dispersion of the LO phonon mode and an additional wave vector with magnitude $G=(2\pi/a)$ provided by a periodic modulation (with lattice constant a) of the electric field associated to the electromagnetic light wave. If this periodic modulation would originate solely from the track-like assembly of the rods, then the LISP peak should also be observable in assemblies of CdS rods. Since this is not the case (see „shell only C tracks" in Fig. 3b), we have to provide a different explanation.

We propose that a grating coupler effect is produced by photo-induced charges localized in the vicinity of the CdSe cores. A similar grating coupler effect induced by electrical charges has been reported in Ref. [27]. Various experimental works demonstrated that for excitation energies below the CdS band gap the photo-excited holes in the dot/rod core-shell nanorods are localized to the CdSe core region, while the electrons are more delocalized over the CdS rod volume. [22-23] Figure 4b illustrates the spatial distribution of the electrons and holes in the core-shell nanorods that results from the different band offsets in the conduction and valence band. We suggest that the photo-induced periodic modulation of charge density in the nanorod assembly leads to the grating coupler effect.

5. Numerical Model

We have calculated with the Comsol Multiphysics software the magnitude of the electric field vector **E** of a plane electromagnetic wave polarized in x-direction and traveling in y-direction at a wavelength of 514 nm in an array with, and without, localized charges. We modeled the shape of the rods with rectangles with an aspect ratio of 5, and attributed the dielectric constants of $\varepsilon_{CdSe}=9.3$ to the core, and $\varepsilon_{CdS}=8.3$ to the shell area[3]. The charge distribution of the photo-generated electrons was approximated by an elliptical area, and the holes were confined in the spherical CdSe core region. The charge density was chosen such that the integral of ρ over the corresponding volume in 3D for holes and electrons equals +/- 1.6 10^{-19} Coulomb, and the charge density C/m^3 was inserted correspondingly.

In detail, in our 2D model we assumed a homogeneous circular distribution of positive charge at the CdSe core, and different elliptical distributions for the electrons as illustrated in Fig. 4d-g by the black lines. The total positive

charge was set equal to the total negative charge in order to match the prerequisite of photo-generated electron-hole pairs. We calculated the electrostatic potential resulting from these charge distributions, and inserted the resulting displacement field **D** into the calculation for the electric field associated to the electromagnetic wave. The obtained results for **E** for different charge distributions within the nanorods are displayed in Fig. 4 d-g. We clearly observe a significant modulation of **E** due to the presence of charged regions (d-f), while in the case of uncharged nanorods (g) the E-Field is more or less constant inside the rod volume. This calculation therefore strongly supports our assumption of a photo-induced grating coupler effect.

6. Conclusions

In conclusion, we observed the CdSe and CdS LO phonon excitations in dot-in-a-rod core-shell nanorods by Raman spectroscopy. Raman spectra recorded from samples with rods ordered into long tracks showed a broad phonon mode slightly red-shifted from the CdS LO phonon energy that could only be observed at wavelengths in resonance with higher CdSe core transitions. We attributed the appearance of this new mode to a light induced grating coupler effect that originated from the different spatial distributions of the photo-excited electrons and holes, and supported this assumption by a calculation of the photo-induced modulation of the electromagnetic light wave field. We think that a photo-induced grating coupler effect could be very interesting not only for exciton-phonon coupling but also for the emerging field of photonic-plasmonic interaction. In particular, it could be exploited for the coupling of nanocrystal emission with surface plasmons in metal nanostructures.

7. References

1. J. T. Hu *et al.*, Science **292**, 2060 (2001).
2. P. E. Trudeau *et al.*, Nano Lett. **8**, 1936 (2008).
3. H. Steinberg *et al.*, Nano Lett. **9**, 3671 (2009).
4. L. Carbone *et al.*, Nano Lett. **7**, 2942 (2007).
5. D. Steiner *et al.*, Phys. Rev. B **80**, 195308 (2009).
6. A. Persano *et al.*, Acs Nano **4**, 1646 (2010).
7. H. E. Romero, G. Calusine, and M. Drndic, Phys. Rev. B **72**, 235401 (2005).
8. D. J. Norris *et al.*, Physical Review B-Condensed Matter **53**, 16347 (1996).
9. Z. X. Sun *et al.*, Phys. Rev. Lett. **102** (2009).
10. C. Trallero-Giner *et al.*, Phys. Rev. B **57**, 4664 (1998).
11. R. Krahne *et al.*, Nano Lett. **6**, 478 (2006).
12. H. Lange *et al.*, Phys. Rev. B **77** (2008).
13. C. Nobile *et al.*, Nano Lett. **7**, 476 (2007).
14. H. Lange *et al.*, Nanotechnol. **20** (2009).
15. G. Chilla *et al.*, Phys. Rev. Lett. **100** (2008).
16. H. Lange *et al.*, Nano Lett. **8**, 4614 (2008).
17. G. D. Mahan *et al.*, Phys. Rev. B **68**, Art. No. 73402 (2003).
18. D. Steiner *et al.*, Nano Lett. **6**, 2201 (2006).
19. D. Steiner *et al.*, Nanotechnol. **19**, art. no. 065201 (2008).
20. R. X. Yan *et al.*, Proceedings Of The National Academy Of Sciences Of The United States Of America **106**, 21045 (2009).
21. A. L. Efros *et al.*, Physical Review B-Condensed Matter **54**, 4843 (1996).
22. M. G. Lupo *et al.*, Nano Lett. **8**, 4582 (2008).
23. A. Sitt *et al.*, Nano Lett. **9**, 3470 (2009).
24. C. Tralleroginer, M. Cardona, and F. Iikawa, Phys. Rev. B **48**, 5187 (1993).
25. Landolt-Boernstein, (Springer-Verlag GmbH, 1998), Vol. 41c.
26. R. Gupta *et al.*, Nano Lett. **3**, 1745 (2003).
27. R. J. Wilkinson *et al.*, J. Appl. Phys. **71**, 6049 (1992).